Atmos. Chem. Phys. Discuss., 4, 2973–2989, 2004
www.atmos-chem-phys.org/acpd/4/2973/
SRef-ID: 1680-7375/acpd/2004-4-2973

Atmospheric
Chemistry
and Physics
Discussions

Rayleigh lidar observation of a warm stratopause over a tropical site, Gadanki (13.5° N; 79.2° E)

V. Sivakumar[1], **B. Morel**[1], **H. Bencherif**[1], **J. L. Baray**[1, 2], **S. Baldy**[1], **A. Hauchecorne**[3], **and P. B. Rao**[4]

[1]Laboratoire de Physique de l'Atmosphère CNRS-UMR 8105, Université de La Réunion, 15 Av. René Cassin, BP 7151, 97715 Saint-Denis Messag. Cedex 9, La Réunion, France
[2]Institut Pierre Simon Laplace (IPSL), Observatoire de Physique de l'Atmosphère de la Réunion (OPAR), La Réunion, France
[3]Service d'Aéronomie du CNRS, UMR 7620, France
[4]National Remote Sensing Agency, Bala Nagar, Hyderabad – 500 037, India

Received: 15 January 2004 – Accepted: 26 March 2004 – Published: 2 June 2004

Correspondence to: V. Sivakumar (siva@univ-reunion.fr)

Abstract

The first Rayleigh lidar observation of a stratopause warming over a tropical site, Gadanki (13.5° N; 79.2° E) is presented in this paper. The warming event has been observed on 22–23 February 2001, and has been found to occur in the stratopause height region (~45–55 km). The magnitude of the warming is found to be ~18 K with respect to the winter-mean temperature profile derived from the lidar data collected over March 1998 to July 2001. The event observed by the lidar has also been seen in the data from Halogen Occultation Experiment (HALOE) on board the UARS satellite. The zonal-mean temperature at 80° N and the zonal-mean zonal wind at 60° N from National Centre for Environmental Prediction (NCEP) and European Centre for Medium-Range Weather Forecasts (ECMWF) reanalysis indicate that a major warming episode also took place in the northern polar hemisphere, a week before to the day of the observation over Gadanki. Eliassen-Palm (E-P) flux calculations from ECMWF reanalysis show evidence of propagation of planetary-wave activity from high and mid to low latitudes consecutive to the major warming episode over the pole. Our results support the view that the most likely source mechanism for the observed stratopause warming is the increase in planetary-wave activity.

1. Introduction

One spectacular transient phenomenon to be observed in the middle atmosphere is the stratospheric sudden warming (SSW). Since the first observation by Scherhag (1952), there have been large numbers of evidence of SSW over the globe, especially in the northern hemisphere. Review articles on SSW include that, for example, by Schoeberl (1978). He noted that sudden warmings would occur mostly in the northern polar hemisphere during wintertime, and that they might be associated with the anomalous growth of the planetary waves (PW) that propagate from the troposphere into the stratosphere during winter. Stratospheric warmings have been classified into major and minor warmings, depending on the amplitude of the temperature perturbations (e.g. Andrews et al., 1987; Donfrancesco et al., 1996; Marenco et al., 1997). Major warmings are characterized by large perturbations of temperature and the reversal of zonal-mean temperature gradients and the zonal-mean wind at 60° N latitude in the mid-stratosphere (at and below 10 hPa). In contrast, minor warmings are characterized by weaker perturbations of temperature and the reversal of the zonal-mean temperature gradients. In recent years, stratospheric warmings have been observed at mid (Hauchecorne and Chanin, 1983) and high latitudes (Whiteway and Carswell, 1994; Donfrancesco et al., 1996; Whiteway et al., 1997; Duck et al., 1998; Walterscheid et al., 2000) using lidar measurements. The cause of such warmings has been interpreted either in terms of gravity-wave (GW) activity (Whiteway and Carswell, 1994; Whiteway et al., 1997), PW activity (Hauchecorne and Chanin, 1983; Marenco et al., 1997) or formation of vortex core and PW breaking (Schoeberl, 1978; Labitzke, 1981; Duck et al., 1998; Walterscheid et al., 2000).

Besides the lidar, satellite and rocket measurements have also been used to report on SSW events (Appu, 1984; Dunkerton et al., 1988; Dunkerton and Delisi, 1986; Delisi and Dunkerton, 1988; Randel, 1993). Using 35 years of satellite data, Dunkerton et al. (1988), found that the occurrence of major SSW events depends on the Quasi-Biennial Oscillation (QBO) phase. They showed that major SSW occurs only when the QBO blows westerly.

Here we describe, using ground-based lidar measurements from the tropical station of Gadanki (13.5° N; 79.2° E), a warming event observed at the stratopause layer on 22–23 February 2001. The observed event is discussed interms of PW and GW activities. To support our observation, we also present data from Halogen Occultation Experiment (HALOE) on board the UARS satellite. Since there has been no such kind of results from a tropical station, we believe that our result is the first of its kind as reported from a tropical station using ground-based lidar measurements.

2. Data and analysis

The lidar data presented in this paper have been collected at the National MST Radar Facility (NMRF), Gadanki (13.8° N, 79.2° E), for the night of 22–23 February 2001 with measurements performed continuously from 20:00 to 02:00 LST. Using the photon count profiles from lidar data and a model atmosphere (MSISE-90), temperature profiles are derived for the height range of 30–90 km following the method of analysis given by Hauchecorne and Chanin (1980). Further details on the system and data analysis can be found in Sivakumar et al. (2001, 2003).

Additionally, we use the UARS-HALOE satellite for comparison together with NCEP and ECMWF reanalysis data to interpret the warming event.

3. Result

3.1. Lidar and satellite observations

The lidar temperature profile for the night of 22–23 February 2001 is shown in Fig. 1 (the red coloured line along with standard deviation). For comparison, the winter-monthly (November, December, January and February) mean temperature profile derived from the lidar data collected over Gadanki from March 1998 to July 2001 (Sivakumar et al., 2003) is also displayed (see legend). The lidar profile for the night of 22–23 February 2001 clearly shows temperature increase in the stratopause region to a maximum value of 283 K around 45 km. The magnitude of warming is found to be ten times larger than the calculated standard deviation (~3 K at 60 km and ~2 K at 50 km). Additionally, the HALOE temperature measured on the same day over the closest location (10.46° N; 73.31° E) is included in Fig. 1 (line with open circles). Agreement between lidar and satellite temperature profiles is generally good. The amplitude of the HALOE temperature maximum (281 K) during the warming event is close to that of the lidar, confirming the accuracy of the event. A discrepancy in the height between lidar (at

45 km) and HALOE (at 46 km) of the warming event is however observed. It may be related to the poorer height resolution for the HALOE measurement (3.7 km) in comparison with that of the lidar (0.3 km).

Figure 2 illustrates the magnitude of the observed warming over Gadanki. This has been obtained by subtracting successively from the 22–23 February profile, temperature values recorded a week before (14–15 February) and a week after (28 February–1 March) by lidar, and by subtracting the climatological profiles derived from lidar and HALOE measurements, as well. In the stratopause height region, the amplitude of warming, is found to be about ∼18 K with respect to the lidar derived mean temperature profiles, and ∼15–16 K for rest of the cases. It appears that the order of magnitude of the stratopause warming observed over Gadanki is smaller than that have been reported for mid and high latitudes in the northern hemisphere (about 30 K) (Hauchecorne and Chanin, 1983; Whiteway and Carswell, 1994; Whiteway et al., 1997; Duck et al., 1998). Moreover, from the time-evolution of daily temperature values obtained at the stratopause during the January-February-March period, both lidar and ECMWF data have a maximum on 22–23 February 2001 (figure not shown).

4. Discussion

One dynamical feature in the lidar temperature profile presented on Fig. 1 is the wave-like structure oscillating around an average profile with amplitude increasing with height. Two systems of waves are primarily responsible for this wave-like structure: planetary waves (PW) and gravity waves (GW).

GW are known to have a profound effect on the thermal and dynamical structure of the middle atmosphere. GW propagating upward from the lower atmosphere grows in response to the decreasing background atmospheric density. When they approach critical levels or when they induce convective instability, they are dissipated, and their associated momentum is deposited into the flow. This process is responsible for the phenomenon known as the mesospheric temperature inversion (Hauchecorne et al., 1987; Leblanc et al., 1995). However, Ratnam et al. (2003) reporting on mesospheric temperature inversions using 40 months of NMRF-lidar observations over Gadanki, have shown that mesospheric temperature inversions at this latitude occur in the height range of 70–80 km, with larger perturbations during summer than winter. Moreover, estimates of the GW potential energy during the lidar measurement period over the night of 22–23 February 2001 show an increase in GW potential energy in the stratopause region up to about 135 $J.kg^{-1}$ at the stratopause height (figure not shown). This increase is however not sufficient to explain a temperature rise of 16–18 K as observed during the event (Sivakumar et al., 2001). As well, the comprehensive study on the middle atmospheric gravity wave activity was shown that the wave activity is at a maximum in winter at high latitudes and in equinoxes at low latitudes (Fritts, 1984). Garcia and Boville (1994) have also noted that the role of GW may not be significant in the northern polar vortex as in the southern polar vortex. Thus, there should be another dynamical source, the PW activity, which may be responsible for the observed warming. This is further explored in the following sub-section.

4.1. PW drive: NCEP and ECMWF reanalyses

Information about the evolution of the stratospheric state at the time of the lidar observation is provided by the NCEP and ECMWF data. The NCEP and ECMWF data are used on a 2.5°×2.5° grid from 1000 to 10 hPa (15 levels) and from 1013.25 to 0.20 hPa (60 levels), respectively. As shown in Fig. 1, the stratopause-warming event can also be seen in the ECMWF data derived for the location and the date of the lidar sounding. The temperature maximum value is found to be close to that observed by the lidar, although located at a higher altitude. The altitude difference may be attributed to the poor vertical resolution of satellite radiances assimilated in ECMWF around the stratopause.

Figure 3a and b shows the NCEP zonal-mean temperature at 80° N and the zonal-mean zonal wind at 60° N at three different pressure levels, i.e. 50, 30 and 10 hPa, for the period extending from 1 July 2000 to 30 June 2001. Examination of Fig. 3a indicates that a minor stratospheric warming occurred during the second half of January 2001 over the polar region, turning into a major warming in mid-February with the reversal of the zonal wind (Fig. 3b). The stratosphere then returned slowly to winter conditions although the circulation remained disturbed up to the beginning of March, so that the time interval for the event was approximately 45 days. It can be seen from Fig. 3 that the warming event observed in the lidar sounding over Gadanki (vertical dotted lines) appears to occur shortly after the peak of temperature and circulation anomalies over the polar region.

Planetary waves (PW) are known to be responsible for bringing about the large mean-flow changes observed during sudden warmings. To gain deeper insights into the dynamical processes occurring during the warming event of February 2001, we use isentropic maps of Ertel's potential vorticity (PV). This approach has been used elsewhere (e.g. McIntyre and Palmer, 1983; Dunkerton and Delisi, 1986) to discuss the dynamics of sudden warming events in connection with breaking planetary waves (PW). In fact, using Nimbus 7 Limb Infrared Monitor of the Stratosphere (LIMS), Dunkerton and Delisi (1986) have studied the time evolution of PV in the winter period from January–February 1979, and suggested that the temporal evolution of the size, shape and orientation of the main circumpolar vortex would be revealed very clearly by the potential vorticity field. The size of the vortex determines the range of latitudes over which planetary and Rossby waves are able to propagate.

Figure 4a and b shows PV maps for the 1900-K isentropic surface representing the stratopause region calculated from the ECMWF reanalyses. The PV-map obtained on 15 February, a week before the stratopause warming over Gadanki, is principally characterized by a tropical air mass (low PV) excursion northward to the polar region, and with a longitudinal extension from 0° to 100° E (see Fig. 4a). The lidar site, indicated on the PV-maps by the symbol "Ga", appears on Fig. 4a nearly under the zero-PV zone. From examination of the PV-map obtained on 22 February, one can notice a "tongue" of high-PV emanating from polar latitudes and extending westward and equator-ward (see Fig. 4b). Meanwhile, it can also be watched from that PV-field an air-mass "intrusion" coming originally from the southern tropical zone (low and negative PV) and moving northward and eastward, with an extension up to 30° N and from ≈20° W to ≈70° E. Thus, the PV-maps give evidence of horizontal exchange between the tropics and high-latitudes. The obtained air-mass exchange induced at the 900-K level to a large surf zone covering the lidar site, and where the PV-lines seem irreversibly twisted (see Fig. 4b), suggesting a process of PW drive and its breaking. Further diagnostics of the planetary-wave activity and possible breaking-wave regimes are provided by the Eliassen-Palm (EP) flux $\boldsymbol{F}$ and the divergence of the EP flux $\nabla.\boldsymbol{F}$, which are expressed in spherical geometry as:

$$\boldsymbol{F} = \left\{F_{(\phi)}, F_{(z)}\right\} = \left\{-\rho_0 a\cos\phi\,\left(\overline{v'u'}\right),\; f\rho_0 a\cos\phi\left(\frac{\overline{v'\theta}}{\overline{\theta}_z}\right)\right\} \qquad (1)$$

and

$$\nabla.\boldsymbol{F} = \frac{1}{a\cos\phi}\left(F_{(\phi)}\cos\phi\right)_{\phi} + \left(F_{(z)}\right)_{z}. \qquad (2)$$

where the overbars and primes denote zonal means and deviations, there from, all other symbols being as in Andrews et al. (1987).

The orientation of the EP flux vector indicates the direction of PW propagation (Kanzawa, 1984; Dunkerton and Delisi, 1986; Delisi and Dunkerton, 1988). Planetary wave activity in the mid latitudes generally propagates from the winter troposphere up into the stratosphere and toward the equator. PW breaking in the EP fluxes can be recognized by the convergence of the EP vectors ($\nabla.\boldsymbol{F}<0$). Figure 5a, b and c displays latitude-altitude cross-sections of the EP flux (arrows) for several days nearby the lidar sounding. Wave fluxes in the vector's formulation are computed using ECMWF data. To allow the EP vectors to be seen clearly throughout the stratosphere, the vectors are multiplied by $e^{z/H}$ (Mechoso et al., 1985). In addition, $F_{(z)}$ is magnified by a factor 150 with respect to $F_{(\phi)}$ (Randel et al., 1987). Superimposed on these figures is the wave driving (shaded and contours) which is proportional to the EP flux divergence: $D=\frac{1}{\rho_0 a\cos\phi}\nabla.\boldsymbol{F}$. As it can be seen from Fig. 6a, on 15 February, a week before the stratopause warming over Gadanki, strong EP flux throughout the middle atmosphere is evident over the high and mid latitude regions. *F* arrows indicate a vertical propagation out of the troposphere into the lower stratosphere, turning then to an equatorward propagation in the upper stratosphere and lower mesosphere region. Here the "focusing" of the waves is accompanied by large negative values of the wave driving *D*, on the order of several tens of meters per second per day and towards poleward of 30° latitude (dashed contours). On 23 February, on day of the stratopause warming (see Fig. 5b) the propagation is getting further equatorward into the tropical region, where the stronger wave activity and convergence of EP flux are likely to produce a rapid deceleration of the zonal-mean zonal wind (leading to the poleward migration of low-latitude easterlies – figure not shown) and the associated temperature rise. One week later (Fig. 5c), the middle atmosphere returns to normal, with planetary-wave activity remarkably weaker and confined to the high-latitude region.

5. Conclusion and additional remarks

This paper reports on the first warming event observed by lidar in the stratopause region over a tropical site (Gadanki, India). The accuracy of the event was confirmed using co-located and quasi-simultaneous temperature data from HALOE on board the UARS satellite. The magnitude of the warming observed by lidar was found to be ∼18 K with respect to the winter monthly-mean temperature profiles derived from the lidar/HALOE data collected over March 1998 to July 2001. The magnitude is less than the values usually reported over mid and high latitude regions in the northern hemisphere (about 30 K) (Hauchecorne and Chanin, 1983; Whiteway and Carswell, 1994; Whiteway et al., 1997; Duck et al., 1998). The warming event over Gadanki appeared to occur shortly after a major stratospheric warming event over the polar region. Using EP flux calculations from ECMWF reanalyses, we found that the event was mainly driven by PW propagating from high and mid to low latitudes consecutive to the major warming episode over the pole. Though the temperature perturbation during the event was too large due only to GW, it is suspected that enhancement in GW activities through interactions with PW and mean flow may have large impacts on the temperature profile. Since, the objective of the paper is to report on the observed event, the expectation of a quadrupole moment between the poles and the tropics (Delisi and Dunkerton, 1988) is not explored. In future, the above issues will be addressed through coupling experimental data with model simulations and quantification tools.

Acknowledgements. The National MST Radar Facility is operated by Department of Space (DOS), Government of India with partial support from Council of Scientific and Industrial Research (CSIR). Authors are thankful to the Upper Atmosphere Research Satellite (UARS) Project, (Code 916), and the Distributed Active Archive Center (Code 902), at the Goddard Space Flight Center, Greenbelt, MD 20771, for providing HALOE satellite data through their web site http://haloedata.larc.nasa.gov/Haloe. Finally, the authors wish to thank the NOAA Climate Diagnostics Center (http://www.cdc.noaa.gov/) for providing portions of the NCEP/NCAR reanalysis data.

Laboratoire de Physique de l’Atmosphère (LPA) is supported by the French Centre National de la Recherche Scientifique (CNRS)/Institut National des Sciences de l’Univers (INSU) and Conseil Régional de la Réunion. One of the authors, V. Sivakumar, acknowledges the CNRS for the financial support under post-doctoral fellowship scheme.

References

Andrews, D. G., Holton, J. R., and Leovy, C. B.: Middle Atmosphere Dynamics, Acad. Press, 1987.

Appu, K. S.: On Perturbations in the Thermal structure of Tropical stratosphere and Mesosphere in Winter, I. Journal of Radio and Space Physics, Vol. 13, 35–41, 1984.

Delisi, D. P. and Dunkerton, T. J.: Seasonal variation of the semiannual oscillation, J. Atmos. Sci., 45, 2772–2787, 1988.

Donfrancesco, G. D., Adriani, A., Gobbi, G. P., and Congeduti, F.: Lidar observations of stratospheric temperature above McMurdo Station, Antartica, J. Atmos. Terr. Phys., 58, 1391–1399, 1996.

Duck, T. J., Whiteway, J. A, and Carswell, A. I.: Lidar observations of gravity wave activity and arctic stratospheric vortex core warming, Geophys. Res. Lett., 25, 2813–2816, 1998.

Dunkerton, T. J. and Delisi, D. P.: Evolution of potential Vorticity in the winter stratosphere of January-February 1979, J. Geophys. Res., 91, 1199–1208, 1986.

Dunkerton, T. J., Delisi, D. P., and Baldwin, M. P.: Distribution of Major Stratospheric warmings in relation to the Quasi-Biennial Oscillation, Geophys. Res. Lett., 15, 136–139, 1988.

Fritts, D. C.: Gravity wave saturation in the middle atmosphere: A review of theory and observations, Rev. Geophys. Space Phys., 22, 275–308, 1984.

Garcia, R. R. and Boville, B. A. : "Downward Control" of the mean meridional circulation and temperature distribution of the polar winter stratosphere, J. Atmos. Sci., 51, 2238–2245, 1994.

Hauchecorne, A. and Chanin, M. L.: Density and temperature profiles obtained by lidar between 35 and 70 km, Geophys. Res. Lett., 8, 565–568, 1980.

Hauchecorne, A. and Chanin, M. L.: Mid latitude observations of planetary waves in the middle atmosphere during the winter over 1981–1982, J. Geophys. Res., 88, 3843–3849, 1983.

Hauchecorne, A., Chanin, M. L., and Wilson, R.: Mesospheric temperature inversion and gravity wave breaking, Geophys. Res. Lett., 14, 933–936, 1987.

Kanzawa, H.: Four observed sudden stratospheric warmings diagnosed by the Eliassen-Palm flux and refractive index, Dynamics of the Middle Atmosphere, Proceedings of a U.S.-Japan Seminar, Honolulu, Hawaii, 8–12 November 1982, edited by Holton, J. R. and Matsuno, T., p. 307–331, 1984.

Labitzke, K.: Stratospheric-mesospheric midwinter disturbances: a summary of observed characteristics, J. Geophys. Res., 86, 9665–9678, 1981.

Leblanc, T., Hauchecorne, A., Chanin, M. L., Taylor, F. W., Rodgers, C. D., and Livesey, N.: Mesospheric temperature inversions as seen by ISAMS (UARS), Geophys. Res. Lett., 22, 1485–1488, 1995.

Marenco, F., di Sarra, A., Cacciani, M., Fiocco, G., and Fua, D.: Thermal structure of the winter middle atmosphere observed by lidar at Thule, Greenland, during 1993–1994, J. Atmos. Solar. Terr. Phys., 59, 151–158, 1997.

McIntyre, M. E. and Palmer, T. N.: Breaking planetary waves in the stratosphere, Nature, 593–600, 1983.

Mechoso, C. R., Hartmann, D. L., and Farrara, J. D.: Climatology and interannual variability of wave, mean-flow interaction in the Southern Hemisphere, J. Atmos. Sci., 42, 2189–2206, 1985.

Randel, W. J., Stevens, D. E., and Stanford, J. L.: A study of planetary waves in the southern winter troposphere and stratosphere, Part II: Life cycles, J. Atmos. Sci., 44, 936–949, 1987.

Randel, W. J.: Global variations of zonal mean ozone during stratospheric warming events, J. Atmos. Sci., 50, 3308–3321, 1993.

Ratnam, M. V., Nee, J. B., Chen, W. N., Sivakumar, V., and Rao, P. B.: Recent observations of mesospheric temperature inversions over a tropical station (13.5° N; 79.2° E), J. Atmos. Solar Terr. Phys., 65, 323–334, 2003.

Scherhag, R.: Die explosionsartige Stratosphärenerwärmung des Spätwinters 1951/52, Ber. Deut. Wetterdienst 38, 51–63, 1952.

Schoeberl, M. R.: Stratospheric warmings: observations and theory, Rev. Geophys. Space Phys., 16, 521–538, 1978.

Sivakumar, V., Bhavanikumar, Y., Raghunath, K., Rao, P. B., Krishnaiah, M., Mizutani, K., Aoki, T., Yasui, M., and Itabe, T.: Lidar measurements of mesospheric temperature inversion at a low latitude, Ann. Geophys., 19, 1039–1044, 2001.

Sivakumar, V., Rao, P. B., and Krishnaiah, M.: Lidar measurements of stratosphere-mesosphere thermal structure over a low latitude: Comparison with satellite data and models, J. Geophys. Res., 108, D11, doi:10.1029/2002JD003029, 2003.

Walterschied., R. A., Sivjee, G. G., and Roble, R. G.: Mesospheric and lower thermosphere manifestations of a stratospheric warming event over Eureka, Canada (80° N), Geophys. Res. Lett., 27, 2897–2900, 2000.

Whiteway, J. A. and Carswell, A. I.: Rayleigh lidar observations of thermal structure and gravity wave activity in the high arctic during a stratospheric warming, J. Atmos. Sci., 51, 3122–3136, 1994.

Whiteway, J. A., Duck, T. J., Donovan, D. P., Bird, J. C., Pal, S. R., and Carswell, A. I.: Measurements of gravity wave activity within and around the Arctic stratospheric vortex, Geophys. Res. Lett., 24, 1387–1390, 1997.

Title Page
Abstract | Introduction
Conclusions | References
Tables | Figures
◀◀ | ▶▶
◀ | ▶
Back | Close
Full Screen / Esc
Print Version
Interactive Discussion

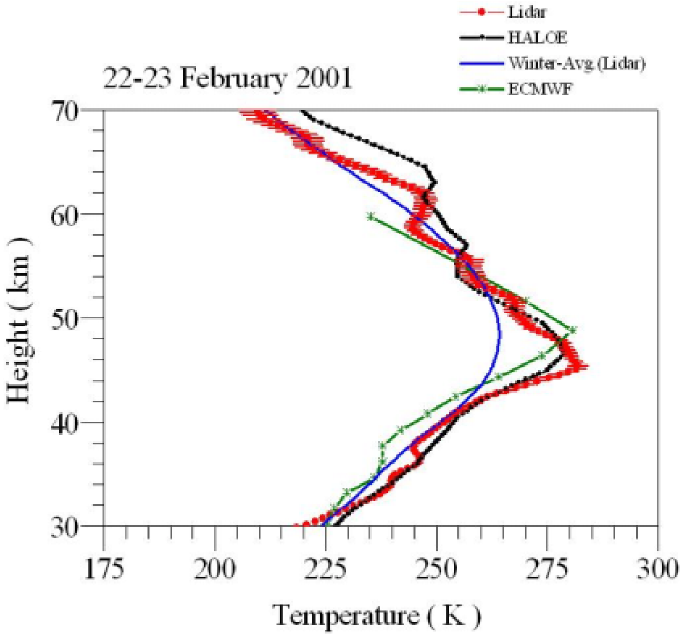

Fig. 1. Temperature profiles of LIDAR, HALOE and ECMWF for the night of 22–23 February 2001, along with the LIDAR mean temperature profile for winter months.

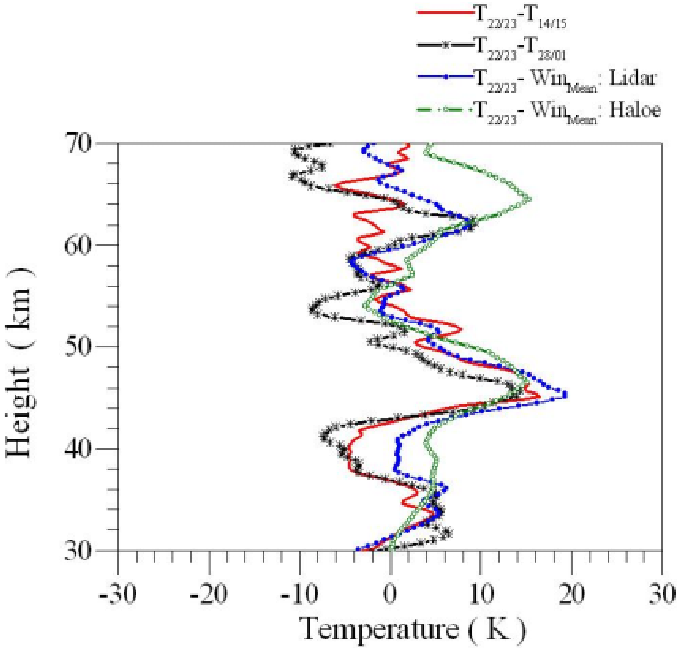

Fig. 2. Temperature difference between the 22–23 February lidar measured temperature profile, a week before, a week after, lidar winter seasonal mean and HALOE seasonal mean profiles. The HALOE climatological profile has been computed by compiling all the winter data recorded from 1998 to 2002, within a discrepancy of ±5° in latitude and ±10° in longitude with regards to the lidar position (13.5° N; 79.2° E).

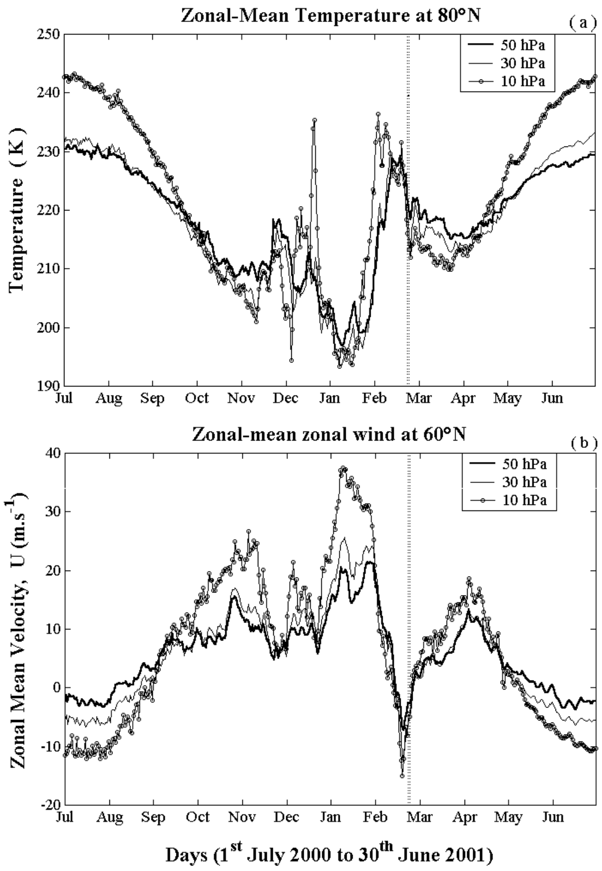

Fig. 3. Variations of **(a)** the zonal-mean temperature at 80° N and **(b)** the zonal-mean zonal wind at 60° N, from 1 July 2000 through 30 June 2001 at 3 different pressure levels in the stratosphere: 50, 30 and 10 hPa, derived from NCEP data. The dotted line indicates the day of the lidar sounding.

Title Page
Abstract
Introduction
Conclusions
References
Tables
Figures
◀▮ ▶▮
◀ ▶
Back
Close
Full Screen / Esc
Print Version
Interactive Discussion

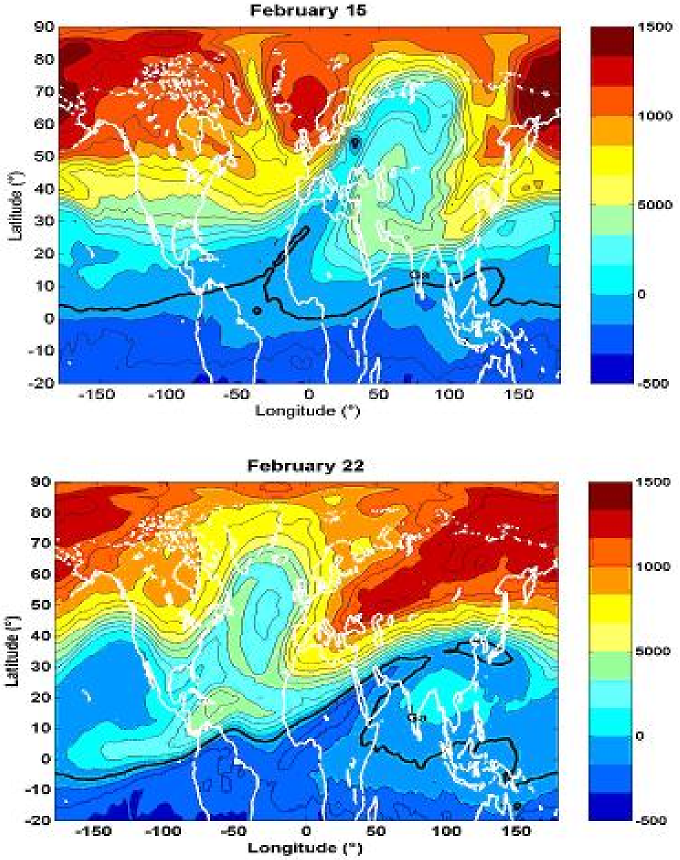

Fig. 4. Evolution of Ertel's Potential Vorticity on the 1900-K isentropic surface for **(a)** 15 February and **(b)** 22 February 2001. The contour interval is 1×10^{-3} K.kg^{-1}.m^{2}.s^{-1} for PV$<10\times10^{-3}$ K.kg^{-1}.m^{2}.s^{-1} (solid lines); it is 5×10^{-3} K.kg^{-1}.m^{2}.s^{-1} for PV$\geq10\times10^{-3}$ K.kg^{-1}.m^{2}.s^{-1} (thick solid lines). "Ga" indicates the location of the lidar station.

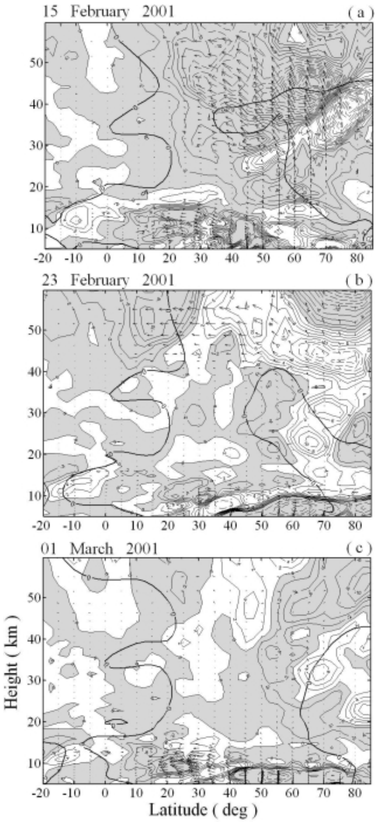

Fig. 5. E-P flux cross-sections in the meridian plane for several days nearby the lidar sounding. Contours represent values of the wave driving term D (see text for definition), in m/s/day; negative wave driving is shaded. The solid and labeled contour stand for the values between -10 and 10 with an interval of 2 m/s/day. The dashed and non-labeled contours stand for the values ≥ 12 and ≤ -12 with the interval of 2 m/s/day for the heights above 15 km and 10 m/s/day for the heights below 15 km.